

Benefits and limitations of imaging multiples: Interferometric and resonant migration

Bowen Guo¹, Jianhua Yu², Yunsong Huang³, Sherif M. Hanafy¹, and Gerard T. Schuster¹

Note: This is the second of two articles in this special section that explore the benefits and limitations of imaging multiples. Also see Hanafy et al., this issue.

Abstract

The benefits and limitations of imaging multiples are reviewed for interferometric migration and resonant migration. Synthetic and field data examples are used to characterize the effectiveness of the methods.

Introduction

This article will review the benefits and limitations for two multiple-imaging methods in exploration and earthquake seismology — interferometric migration and direct migration of multiples. Thinking of multiples as signal instead of noise is an accepted practice in earthquake seismology but is a relatively new concept in exploration seismology. However, multiple reflections from the flat mirror at the ocean's surface allow us to take extra looks at the subsurface. Suitably harnessed, these multiple views have the potential to significantly enhance our characterization of the subsurface. This is especially true if surveys are designed to optimize the use of both primaries and multiples.

Interferometric migration

Interferometric migration can transform VSP ghost reflections into surface-seismic profile (SSP) primaries as if they were virtually recorded at the surface (Figure 1). Unlike mirror migration, no mirror-velocity model is required, and the raypath of the virtual primary in Figure 1c is shorter than the one for mirror migration. Instead of the narrow illumination zone of VSP primaries, interferometric VSP migration illuminates an area almost as wide as an SSP experiment.

Several steps to interferometric migration of multiples (Yu and Schuster, 2006) are recorded by a VSP survey:

- 1) Separate the downgoing and upgoing events in the VSP data by f - k or median filtering. Denote the traces with downgoing arrivals as $d(C, t|A)$ for a surface source at **A** and a receiver in the well at **C** in Figure 1a. The listening-time variable is t , and the excitation is assumed to be at time 0.
- 2) Select a source position at **A** and a virtual receiver point at **B** on the recording surface. Correlate the trace $d(C, t|A)$ with $d(C, t|B)$ and stack the

resulting correlogram over different receiver positions at **C** to obtain the redatumed trace $d(B, t|A)$:

$$d(B, t|A) \approx \sum_C \dot{d}(C, t|B) \otimes d(C, t|A), \quad (1)$$

where the dot denotes the time derivative, the time variable is silent, and \otimes denotes the correlation operation. The trace $d(C, t|A)$ should contain only the downgoing ghosts, but cross-talk noise can be reduced significantly by restricting $d(C, t|A)$ and $d(C, t|B)$ to contain only the first-order downgoing ghost and the direct arrival, respectively. (In this case, only the first-order ghost will be migrated, which is similar to mirror imaging except that the interferometric image is not as sensitive to velocity-model errors, and the receiver's statics are eliminated.)

The physical interpretation of equation 1 is shown in Figure 1, where a VSP multiple is transformed into an SSP primary. In principle, interferometry (Wapenaar and Fokkema, 2006) can transform all N th-order free-surface multiples into lower-order events. For comparison, mirror migration typically transforms only the first-order multiple into a mirror primary with a longer raypath that is more sensitive to migration velocity errors.

- 3) Migrate $d(B, t|A)$ to obtain the subsurface reflector image.

A significant benefit of interferometry is a much wider illumination compared with conventional imaging for a limited source-receiver aperture. This is similar to the merit of migrating receiver functions in earthquake seismology. However, the main limitation is that there will be strong artifacts in the virtual data (and

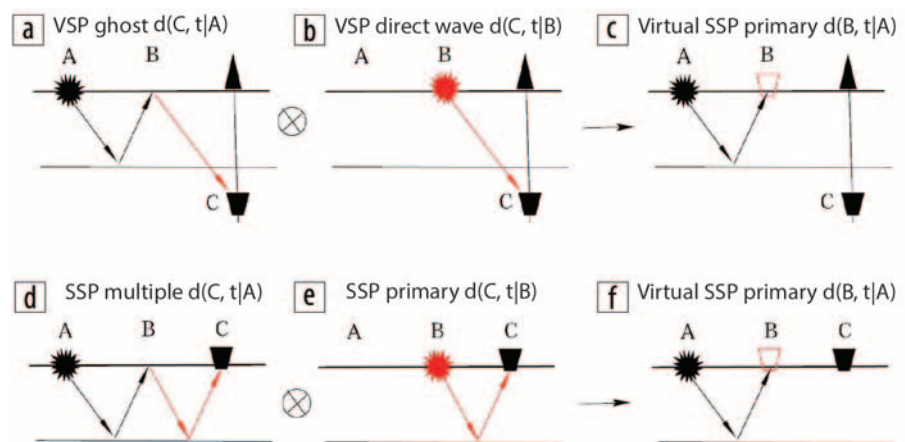


Figure 1. Correlation of the (a) VSP ghost $d(C, t|A)$ with the (b) direct wave $d(C, t|B)$ recorded at **C** gives the (c) virtual SSP primary $d(B, t|A)$ at **B**. Here, the phase associated with the common raypath (red ray) is removed after correlation to give the virtual primary at **B**. Illustrations (d) through (f) are the same except that the input data are SSP primaries and multiples, and the output is a virtual primary trace $d(B, t|A)$. The key principle in interferometric redatuming is the following: Phases associated with the common red raypaths in parts (a) and (b) or parts (d) and (e) cancel one another after correlation to give the remaining phase in the part (c) or part (f) ray. This cancellation also includes any statics at **C**.

¹King Abdullah University of Science and Technology (KAUST).
²BP.

³CGG.
<http://dx.doi.org/10.1190/tle34070802.1>

consequently the interferometric image) unless there is a sufficiently wide source-and-receiver coverage.

A partial remedy to these artifacts is multidimensional deconvolution (Wapenaar et al., 2008), which is a least-squares approach to interferometric redatuming. Interferometry assumes a lossless medium, so attenuation compensation or multidimensional deconvolution should be applied to data with strong attenuation losses.

Figure 2 compares the standard and interferometric migration images generated from acoustic VSP data computed with a Ricker-source wavelet peaked at 15 Hz (Yu and Schuster, 2006). In this example, random statics (with a maximum statics of 15 ms) were applied to the traces. The interferometric-migration image in Figure 2b has a much wider subsurface illumination at the shallow depths than seen in the Figure 2a primary image.

Interferometric migration also is applied to RVSP data recorded by Exxon with 24 geophones on the surface and 98 sources in a Friendswood, Texas, well. The data were processed, and then interferometric migration was applied to the correlated records. The standard- and interferometric-migration images are shown in Figures 2d and 2e, where the interferometric image shows better reflector continuity and wider illumination than the primary migration image does. Source statics were known to be present in the wells and were eliminated automatically by the crosscorrelation operation (see the caption of Figure 1).

Migration of multiples for SSP is recognized (e.g., Berkhout and Verschuur, 1994; Guitton, 2002; Lu et al., 2014) to give a greater subsurface illumination for a limited source-receiver geometry (Figure 3). However, there is the nagging problem of cross talk where the correlation of arrivals with uncommon raypaths can generate unphysical events with strong amplitudes. Migrating these unphysical events can lead to severe coherent noise in the migration image. This problem can be mitigated if there are sufficient fold, effective multiple separation, and wide azimuthal coverage.

As an example, Lu et al. (2014) apply separated wavefield imaging to create common-angle gathers with offset migration in the subsurface-offset domain. Imaging of multiples improves the angle gathers in the coarser sampled direction, e.g., 90° azimuth, for their wide-azimuth data set. According to Lu et al. (2014, p.3930), “the multiples angle gathers prove to be denser and less affected by coarse source sampling than the primaries angle gathers. The finely sampled angle domain image gathers can be used for tomography and pre-stack post processing to improve the overall quality of depth migration.” Migration artifacts also can be eliminated in common-angle gathers (Wang et al., 2014).

The wider coverage of multiples also allows for interpolation methods that can fill gaps in the recording array. For example, note that the bounce point at **A** is not illuminated by a primary in Figure 3a but is illuminated by the multiple in Figure 3b. Interferometry

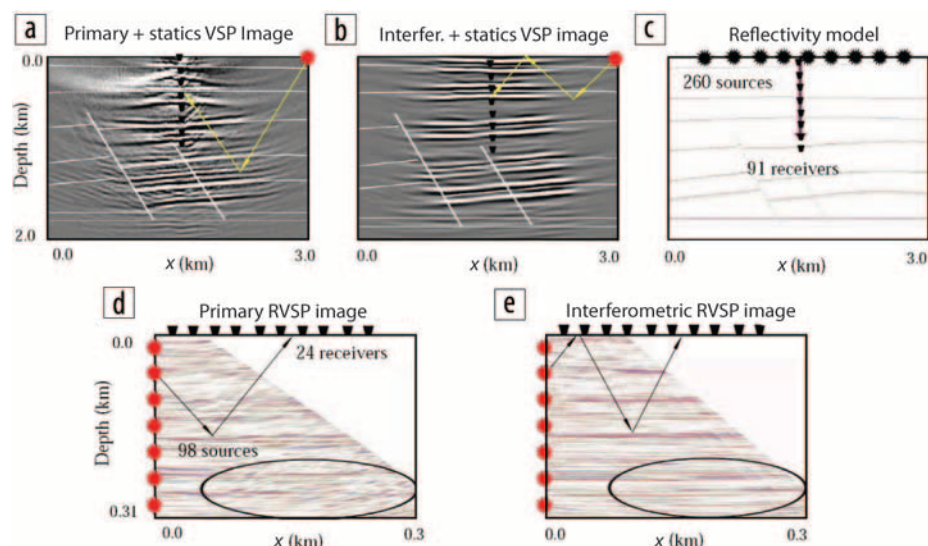


Figure 2. Top row is for synthetic VSP data and bottom is for RVSP field data. The synthetic reflectivity model is in part (c), along with the acquisition parameters. The source and receiver sampling intervals are both 10 m for the top row and 3.3 m for the bottom row of VSP data. In both cases, the interferometric-migration images in parts (b) and (e) show wider illumination zones, better reflector continuity, and more robustness with regard to well statics than the primary migration images do.

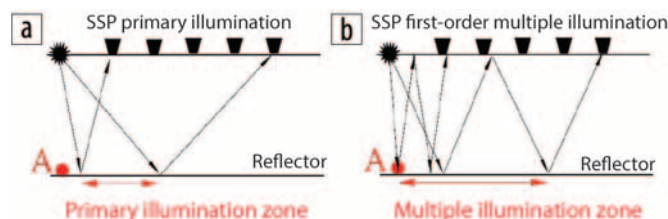


Figure 3. CSG illumination zone for (a) primaries is narrower than that for (b) first-order multiple reflections.

can transform this multiple that reflected at **A** into a primary (Wang et al., 2009; Wang et al., 2010), which can be important for marine surveys that cannot locate a hydrophone close to the source.

Surface-wave inversion and migration

Rayleigh waves in layered media can be described as guided body waves that consist of PS, PP, SS, and SP reverberations. These multiple reflections interfere with one another to satisfy the boundary conditions at the interfaces and so propagate horizontally and evanesce in depth. Earthquake seismologists invert these surface waves for the subsurface S-wave velocity and migrate the backscattered reverberations for near-surface impedance discontinuities (Snieder, 1988).

As an example, more than 5200 passive seismometers were deployed in Long Beach, California, to record more than three weeks of ambient noise (Lin et al., 2014). The records were correlated with one another and were stacked to compute approximate Green's functions at each receiver. The fundamental mode of the surface wave was inverted to give the S-velocity tomogram shown in Figure 4b. In addition, the backscattered surface waves were migrated by Abdullah AlTheyab to give the Figure 4a migration image along the surface.

Note that some of the sharp features in the migration image roughly correlate with the sharp color transitions in the tomogram. This is not surprising because sharp transitions of velocity can correspond to fault scarps that separate one rock type from another.

For exploration geophysics, the combined interpretation of surface-wave tomograms and migration images can pinpoint areas of strong statics as well as potential hazardous regions for drilling (de Ridder et al., 2014).

Migration of resonant multiples

Is it possible to achieve subwavelength (i.e., superresolution) imaging of reflector boundaries in the far field of the sources and receivers? The answer is yes, both in theory and practice with resonant multiples.

Here we define a resonant multiple as a multiple in which the upgoing and downgoing raypaths coincide (Figure 5). For example, the offset between the source and receiver in Figure 5a is zero so that the N th-order free-surface multiple has a travel-time described by

$$T = 2(N + 1)z/V, \quad (2)$$

where $z = d$ is the thickness of the layer, V is the velocity of the topmost layer, and $N = 0$ for a primary reflection. The vertical resolution in locating the depth of the interface can be estimated by first taking the Fréchet derivative of equation 2 with respect to z to obtain

$$\frac{\delta T}{\delta z} = \frac{2(N + 1)}{V}. \quad (3)$$

Defining the dominant period by T_0 , substituting $\delta T \rightarrow T_0/2$ and $\lambda = VT_0$ into equation 3, and rearranging gives the vertical resolution limit $\delta Z \rightarrow \Delta Z$:

$$\Delta z = \frac{\lambda}{4(N + 1)}. \quad (4)$$

This limit says that Δz is the minimum separation in depth between two reflectors that are distinguishable from each other in the data. The greater the order N of the resonance, the better the resolution in depth. If the bed is tilted with respect to the horizontal recording surface, then this resolution limit is along the direction perpendicular to the interface shown in Figure 5b. Guo et al. (2015) extend this concept to subwavelength imaging of dipping reflectors.

Guo et al. (2015) extract first-order resonant multiples from a marine data set and migrate them. To enhance the signal-to-noise ratio (S/N) of the resonant multiples, the traces are resorted into common-midpoint gathers, and then moveout correction aligns the preresonant multiples with the zero-offset resonant multiples. These traces are stacked together to give the enhanced first-order resonant multiples. The primary reflections also are migrated, and the images are compared (Figure 6). Red arrows show that the reflector boundaries have about twice the vertical resolution as the primary reflections do.

The separation of resonant multiples from primaries is imperfect and thus leads to false reflectors, indicated by green arrows in Figure 6a. The removal of these artifacts is a topic for future research.

Summary

The benefits and limitations are reviewed for two multiple-imaging methods in exploration and earthquake seismology — interferometric migration and direct migration of multiples. Imaging multiples can provide some of the following benefits:

- 1) It can illuminate subsurface areas that are not easily accessible to primary reflections recorded by limited source-receiver geometries. In some cases such as in VSP surveys, multiple migration can illuminate blind zones associated with primary migration.
- 2) Trapped reverberations in the near surface, such as surface waves and guided waves, can be inverted for subsurface S-velocities and impedance boundaries. This near-surface information can be used for statics and assessment of drilling hazards.

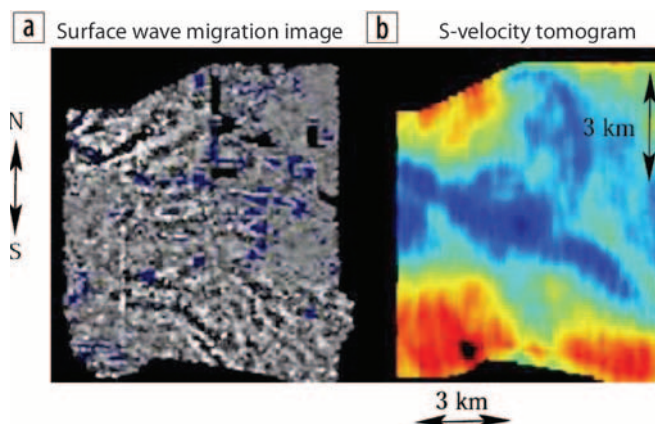


Figure 4. Horizontal slices of the (a) surface-wave migration image at the surface. (b) S-velocity phase tomogram (Lin et al., 2014) reconstructed from Long Beach, California, passive-array data. The image in part (a) is courtesy of Abdullah AlTheyab.

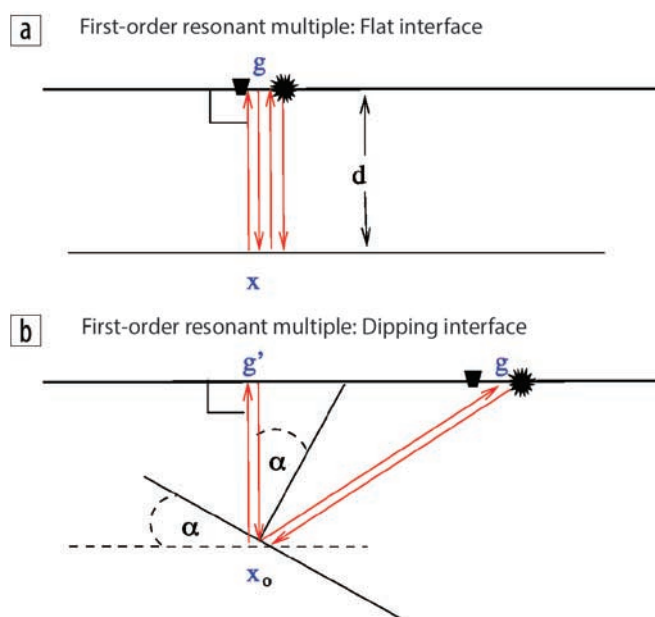


Figure 5. Ray diagrams for first-order resonant multiples in (a) a flat-interface model and (b) a dipping-interface model. The star and quadrilateral represent, respectively, the source and receiver for a zero-offset recording configuration on the earth's free surface.

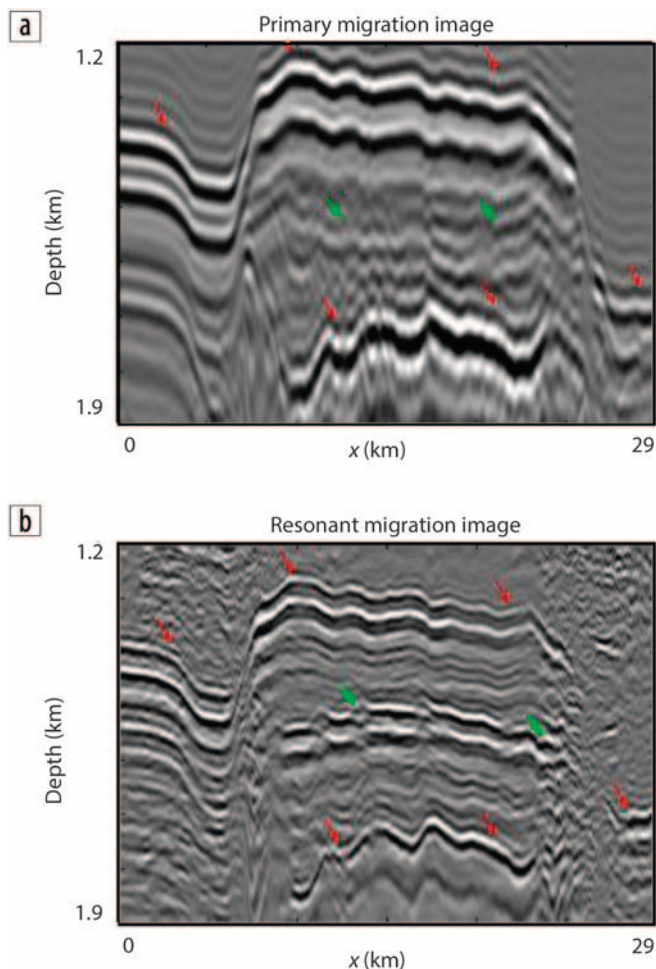


Figure 6. Migration images computed from (a) primary reflection data and (b) stacked resonant multiples. Red arrows mark the true horizon, and green arrows mark the false horizon.

- 3) The migration image from multiples can be stacked to that from primaries to enhance the signal-to-noise ratio in the composite image.
- 4) In some cases, subwavelength imaging of resonant multiples can be achieved in the far field of the sources and receivers.

The major limitations of multiple imaging are the following:

- 1) Strong cross-talk noise associated with the correlation of arrivals without common raypaths will give rise to strong coherent noise in the final interferometric migration image. Partial remedies for this problem include multidimensional deconvolution, wider source-receiver apertures, and denser source and receiver spacing.
- 2) There will be an incomplete transformation of multiples into virtual primaries if the source-receiver aperture is inadequate. This also gives rise to artifacts in the final image.
- 3) Multiples can sometimes give an unreliable AVO signature because the recorded multiple is a product of more than one reflectivity coefficient. In principle, this is not a problem with first-order mirror migration or interferometric imaging.
- 4) The migrated multiple image can be more sensitive to velocity errors and attenuation compared with migration of primaries.

Thinking of multiples as signal instead of noise is an accepted practice in earthquake seismology but is a relatively new concept in exploration seismology. This is somewhat surprising because multiple reflections from the flat mirror at the ocean's surface allow us to take extra looks at the subsurface. Suitably harnessed, these multiple views have the potential to significantly enhance our characterization of the subsurface. This is especially true if surveys are designed to optimize the use of both primaries and multiples. **■**

Corresponding author: gerard.schuster@kaust.edu.sa

References

- Berkhout, A. J., and D. J. Verschuur, 1994, Multiple technology: Part 2, Migration of multiple reflections: 64th Annual International Meeting, SEG, Expanded Abstracts, 1497–1500, <http://dx.doi.org/10.1190/1.1822821>.
- de Ridder, S. A. L., B. L. Biondi, and R. G. Clapp, 2014, Time-lapse seismic noise correlation tomography at Valhall: *Geophysical Research Letters*, **41**, no. 17, 6116–6122, <http://dx.doi.org/10.1002/2014GL061156>.
- Guitton, A., 2002, Shot-profile migration of multiple reflections: 72nd Annual International Meeting, SEG, Expanded Abstracts, 1296–1299, <http://dx.doi.org/10.1190/1.1816892>.
- Guo, B., Y. Huang, and G. Schuster, 2015, Superresolution by moveout correction and migration of surface-related resonant multiples: 77th Conference and Exhibition, EAGE, Extended Abstract, WS06-A02.
- Lin, F.-C., D. Li, R. W. Clayton, and D. Hollis, 2014, High-resolution 3D shallow crustal structure in Long Beach, California: Application of ambient noise tomography on a dense seismic array: *Geophysics*, **78**, no. 4, Q45–Q56, <http://dx.doi.org/10.1190/geo2012-0453.1>.
- Lu, S., N. D. Whitmore, A. A. Valenciano, and N. Chemingui, 2014, Illumination from 3D imaging of multiples: An analysis in the angle domain: 84th Annual International Meeting, SEG, Expanded Abstracts, 3930–3934, <http://dx.doi.org/10.1190/segam2014-0852.1>.
- Snieder, R., 1988, Large-scale waveform inversions of surface waves for lateral heterogeneity: 1. Theory and numerical examples: *Journal of Geophysical Research: Solid Earth*, **93**, no. B10, 12055–12065, <http://dx.doi.org/10.1029/JB093iB10p12055>.
- Wang, Y., S. Dong, and Y. Luo, 2010, Model-based interferometric interpolation method: *Geophysics*, **75**, no. 6, WB211–WB217, <http://dx.doi.org/10.1190/1.3505816>.
- Wang, Y., Y. Luo, and G. T. Schuster, 2009, Interferometric interpolation of missing seismic data: *Geophysics*, **74**, no. 3, SI37–SI45, <http://dx.doi.org/10.1190/1.3110072>.
- Wang, Y., Y. Zheng, X. Chang, and Z. Yao, 2014, Least-squares data to data migration: 84th Annual International Meeting, SEG, Expanded Abstracts, 3951–3955, <http://dx.doi.org/10.1190/segam2014-1151.1>.
- Wapenaar, K., and J. Fokkema, 2006, Green's function representations for seismic interferometry: *Geophysics*, **71**, no. 4, SI33–SI46, <http://dx.doi.org/10.1190/1.2213955>.
- Wapenaar, K., J. van der Neut, and E. Ruigrok, 2008, Passive seismic interferometry by multidimensional deconvolution: *Geophysics*, **73**, no. 6, A51–A56, <http://dx.doi.org/10.1190/1.2976118>.
- Yu, J., and G. T. Schuster, 2006, Crosscorrelogram migration of inverse vertical seismic profile data: *Geophysics*, **71**, no. 1, S1–S11, <http://dx.doi.org/10.1190/1.2159056>.